Medical Physics 386:
The Physics of Medical Imaging 1
X-ray Imaging Notes

5   Image Interpretation   22

6   Conclusion   23

(Last updated: June 15, 2018)

1 Introduction

There are many different imaging modalities in the radiology department— mammography, computed radiography, digital radiography, fluoroscopy, computed tomography (CT), magnetic resonance imaging (MRI), positron-emission tomography (PET), single-photon emission tomography (SPECT), ultrasound, and more. Why are there so many modalities? Because no single modality is optimal for the wide variety of imaging tasks that arise when we try to diagnose disease. Each imaging task has different imaging requirements, so no single modality can be used for all tasks.

A major goal of an imaging medical physicist is to choose and optimize the imaging modality that maximizes the diagnostic content of the image while minimizing cost. This is not a simple task—diagnostic content depends on each specific task, and cost depends on the equipment price, the number of patients that can be imaged per unit time, the radiologists interpretation time, the cost of the exam to the patient, the risks to the patient, the consequences of a false negative exam, the cost of a false positive exam, and more.

One way to understand a medical physicist's task is to examine the relationship between cost, image quality, and diagnostic accuracy. If we assume that there is a monotonic relationship between image quality and diagnostic accuracy (Figure XXX), and if we assume that there is a similar relationship between image quality and cost (Figure XXX), then

In this part of the course, you will learn how to quantify image quality and how it is affected by various acquisition parameters. First, we will review the mathematics required and discuss common image quality metrics. Second, we will discuss x-ray imaging physics and learn how to optimize x-ray imaging systems using the previously developed metrics. Finally, we will discuss the interpretation of the x-ray images and how our interpretation fits into the broader context.

These notes draw heavily from...

Our main reference will be [1].

2 X-ray Imaging

2.1 Basics

We can create an x-ray imaging system by assembling an x-ray **source**, an **object**, and a **detector**. In this section, we will give a brief review of x-ray production, the relevant interactions that take place along the imaging chain, and we will conclude with a basic imaging model.

2.1.1 Sources and Interactions

Brief intro to x-ray production (tubes, anodes, kVp, mA, fluence, etc.)

Brief review of interactions in x-ray energy regime, definition of primary vs. scatter, etc.

2.1.2 Basic Imaging Model

Figure 1 shows a simple example of an x-ray imaging system—we place an x-ray fluence ϕ_0 incident on an object with two attenuation coefficients μ_1 and μ_2. Note that we use bold symbols to indicate random variables. X-rays
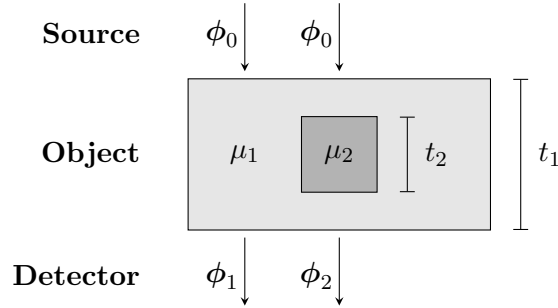
Figure 1: Simplified x-ray imaging schematic. A collimated beam of x-rays with fluence ϕ_o is incident on an object with two attenuation coefficients. A detector measures the output fluences $\phi_{1,2}$.

are attenuated as they pass through the object so the exit fluences are related to the input fluence by

$$\phi_1 = \phi_0 e^{-\mu_1 t_1} \tag{2.1}$$

$$\phi_2 = \phi_0 e^{-\mu_1(t_1 - t_2) - \mu_2 t_2}. \tag{2.2}$$

When we place a detector in the path of the exit beam we create an image of the object.

We will examine more realistic sources and detectors in later sections, but the simple example in Figure 1 is sufficient for us to model image quality in x-ray imaging systems.

2.2 Rose Model

Suppose that we'd like to detect the presence or absence of the small object with attenuation μ_2 in Figure 1 with our imaging system. How well can we perform this task? What conditions do we need to meet to confidently say that the object is present or absent? How should we design our imaging system to meet these conditions? The Rose model supplies answers to these questions and gives us a solid framework for understanding image quality.

First, we define the **signal** S as the mean number of photons blocked by the object

$$S \equiv A(\mathrm{E}\{\phi_1\} - \mathrm{E}\{\phi_2\}) = A\Delta\phi \tag{2.3}$$

where A is the cross sectional area of the object, $\mathrm{E}\{\cdot\}$ denotes the expectation value, ϕ is the x-ray fluence in units of photons per unit area, and $\Delta\phi \equiv \mathrm{E}\{\phi_1\} - \mathrm{E}\{\phi_2\}$. This may seem like a peculiar way to define the signal—shouldn't the signal be the measured intensity difference between areas with and without the object? The reason for our definition is that it captures the role of object size in detectability. Intuitively, larger objects are easier to detect, so our definition of signal should reflect this.

Next, we consider the **noise** N that corrupts our signal. Note that in signal-to-noise ratio discussions the word "noise" usually refers to the standard deviation of a random variable. We will use this meaning. In general the word "noise" refers to any random or unwanted signals.

We define the noise as the standard deviation of the number of photons detected in an area the size of the object when the object is absent.

$$N \equiv \sqrt{\mathrm{Var}\{A\phi_1\}}. \tag{2.4}$$

$A\phi_1$ is a Poisson-distributed random variable, so its variance is identical to its mean

$$N = \sqrt{\mathrm{E}\{A\phi_1\}} \tag{2.5}$$
$$N = \sqrt{A\mathrm{E}\{\phi_1\}}. \tag{2.6}$$

Finally, the signal-to-noise ratio is given by

$$\mathrm{SNR} \equiv \frac{S}{N} = \frac{A\Delta\phi}{\sqrt{A E\{\phi_1\}}}, \tag{2.7}$$
$$\mathrm{SNR} = C\sqrt{A\bar{\phi}}, \tag{2.8}$$

where C is the radiation contrast

$$C = \frac{\Delta\phi}{\bar{\phi}}. \tag{2.9}$$

This is the SNR for an ideal detector where we've assumed that there is

- complete absorption of incident quanta

- no added noise

- no loss of spatial resolution (i.e., no blurring)

2.3   Linear Systems Model of Transmission Radiography

In this section, we aim to devise a mathematical model to describe transmission radiography. Specifically, we would like to use linear systems theory to describe the final radiographic image as a convolution of the object with a point spread function (PSF) contributed by both the x-ray source and the detector.
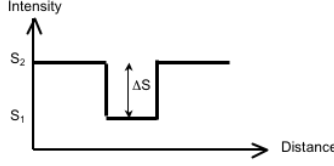
Figure 2: Test

To begin, we consider a simplified geometric representation of an x-ray system, shown in Figure 3, and a few simplifying assumptions:

- we have a 2D, planar, isotropic source, far from the detector plane ($\theta \approx 0$)

- we have a 2D planar object, which does not introduce scattered radiation

- we have an ideal detector, which perfectly detects every photon it encounters
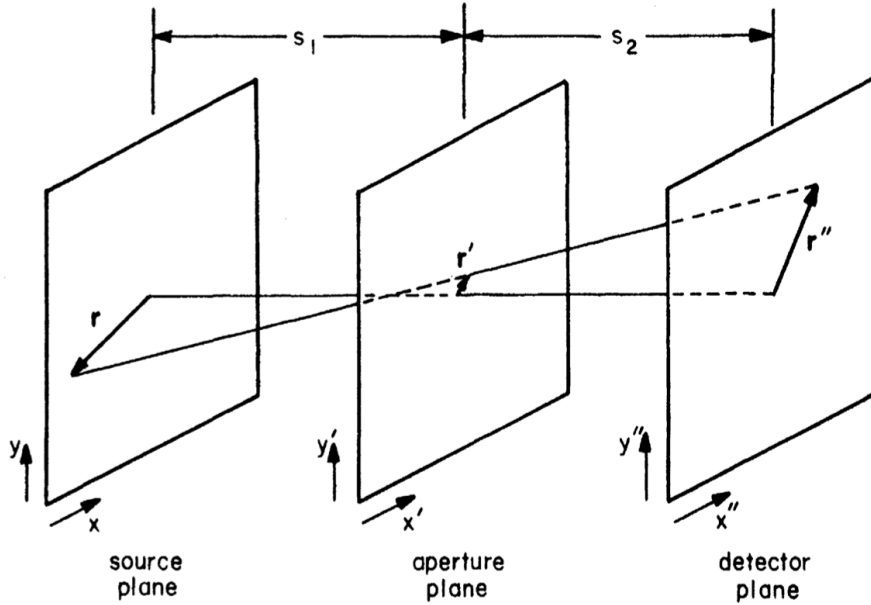
Figure 3: Simplified geometry of a radiographic imaging system. Note: we will refer to the central plane as the "object plane," not "aperture plane," as it appears here.

X-rays are generated at the anode of an x-ray tube, located in the **source plane** (with an elemental area at coordinate r). They then pass through the **object plane** (with an elemental area at coordinate r'), before being detected at the **detector plane** (with an elemental area at coordinate r''). The distance between the source and object planes is s_1, and the distance between the object and detector planes is s_2. It's worth noting that r and r'', which determines r' through the line of sight, are completely general, in the sense that there is nothing special about these vectors. None of r, r'', and r' necessarily ends at the origin of their respective plane. Our goal is to derive an expression for the density of detected photons in the detector plane, $h(r'')$, such that $h(r'')d^2r''$ is the mean number of photons intercepted by the detector area d^2r'' in a time of length T, which we recognize is our image of the object.

4

Clearly, there are a number of idealizations in this setup. We model the 3D anode, the 3D object, and the 2D detector as 2D parallel planes. But we have a path for modeling a realistic system. The 3D anode can be modeled as a series of contiguous parallel planes, and so can the 3D object. Out goal here is to learn important insights from this simplified model.

2.3.1 The Source Plane

We describe the source by an *emission function* $f(\boldsymbol{r})$, where $\boldsymbol{r}$ is the two-dimensional vector in the source plane. The emisison function has units of fluence rate: (photons / unit time · unit area). Thus, the quantity $f(\boldsymbol{r})d^2r$ is the *mean* number of photons per unit time emitted into all space from an elemental area d^2r located at the point $\boldsymbol{r}$. This assumes that the source emits photons isotropically. However, bremsstrahlung photons have a definite preferred orientation which depends on electron energy, angle of electron incidence, and target material. It is possible to incorporate this anisotropy if we modulate $f(\boldsymbol{r})$ by the emission orientation distribution function. We omit that here.
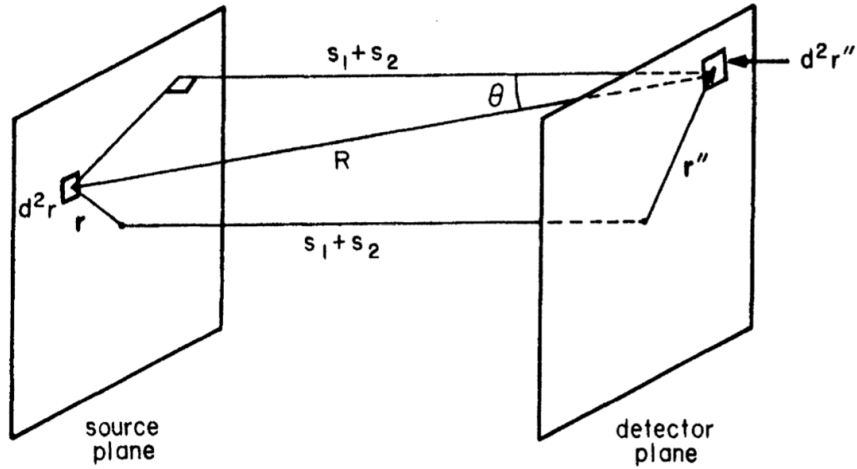
Figure 4: Diagram for solid-angle calculation.

2.3.2 The Detector Plane

Now, let us consider an elemental detector of area $d^2\boldsymbol{r}''$, where $\boldsymbol{r}''$ is the two-dimensional position vector in the detector plane. We can calculate the solid angle $d\Omega$ subtended by the elemental detector area from the source as:

$$d\boldsymbol{\Omega} = \frac{d^2\boldsymbol{r}'' \cdot \cos\theta}{R^2},\tag{2.10}$$

where R is the distance from the source element to the detector element and θ is the angle between the normal to the detector surface and the line of sight from source to detector, as shown in Figure 4. From simple geometry, we know that

$$R = (s_1 + s_2)/\cos\theta,\tag{2.11}$$

5

so we can rewrite Equation 2.10 as

$$d\mathbf{\Omega} = \frac{\cos^3\theta}{(s_1 + s_2)^2}d^2\mathbf{r''}. \tag{2.12}$$

Since a full sphere subtends 4π steradians, the detector element would intercept a fraction $d\mathbf{\Omega}/4\pi$ of the radiation emitted from the source element at location $\mathbf{r}$–in the absence of absorbing material in the object plane at location $\mathbf{r'}$. Thus, the mean number of photons per unit time (1) emitted by the area element $d^2\mathbf{r}$ at location $\mathbf{r}$ in the source plane and (2) intercepted by the area element $d^2\mathbf{r''}$ at location $\mathbf{r''}$ in the detector plane would be

$$f(\mathbf{r})d^2\mathbf{r}\frac{d\mathbf{\Omega}}{4\pi} = f(\mathbf{r})\frac{\cos^3\theta}{4\pi(s_1 + s_2)^2}d^2\mathbf{r}d^2\mathbf{r''}. \tag{2.13}$$

For now, we are assuming an ideal, continuous detector that detects all photons that intercept it. We will lift this restriction shortly; in general, we will see that the detector should be considered an integral part of the imaging system.

2.3.3 The Object Plane

We now consider the effect of the object. We introduce another restriction that we are only dealing with *primary* x-rays; we will discuss the effect of scattered radiation later. A ray emanating from point $\mathbf{r}$ and striking the detector at point $\mathbf{r''}$ will have passed through the object plane at point $\mathbf{r'}$ through the line of sight. We define $g(\mathbf{r'})$ as the transmittance, or the fraction of photons that pass through the object plane at point $\mathbf{r'}$.

We are now in a position to write down an expression for $h(\mathbf{r''})$, the density of detected photons, such that $h(\mathbf{r''})d^2\mathbf{r''}$ is the mean number of photons intercepted by the detector area $d^2\mathbf{r''}$ in a time T. We are not interested in where exactly in the source the photons come from, so we integrate over the entire source plane:

$$h(\mathbf{r''})d^2\mathbf{r''} = \frac{Td^2\mathbf{r''}}{4\pi(s_1 + s_2)^2}\int_{\text{source}} d^2\mathbf{r}\,\cos^3\theta f(\mathbf{r})g(\mathbf{r'}). \tag{2.14}$$

$h(\mathbf{r''})$ has dimensions of fluence (photons per unit area), though we refer to $h(\mathbf{r''})$ as a *photon density* instead, as that term is more appropriate to a static pattern of recorded photons.

We now try to write Equation 2.14 without the use of $\mathbf{r'}$. That is, we will try to write our image not in terms of the object plane, only in terms of the source plane and image plane.

Looking closely at the geometry of Figure 3, we see that

$$\frac{\mathbf{r'} - \mathbf{r}}{s_1} = \frac{\mathbf{r''} - \mathbf{r'}}{s_1 + s_2}, \tag{2.15}$$

where the vectors on the left-hand side are evaluated in the object plane and the vectors on the right-hand side are evelauted in the image plane. Equivalently:

$$\mathbf{r'} = \frac{s_2}{s_1 + s_2}\mathbf{r} + \frac{s_1}{s_1 + s_2}\mathbf{r''} = a\mathbf{r''} + b\mathbf{r}, \tag{2.16}$$

6

evaluated in the object plane and where

$$a = \frac{s_1}{s_1 + s_2} \qquad\qquad b = \frac{s_2}{s_1 + s_2} = 1 - a. \qquad (2.17)$$

Now we can eliminate the vector $\boldsymbol{r}'$. Note that Equations 2.15 and 2.16 describe 2D (not 3D!) vector subtractions in the parallel (x', y') and (x'', y'') planes. The 3D distance R would be written

$$R = \sqrt{|\boldsymbol{r} - \boldsymbol{r}''|^2 + (s_1 + s_2)^2}. \qquad (2.18)$$

With Equation 2.16, we rewrite Equation 2.14 without the use of $\boldsymbol{r}'$ as

$$h(\boldsymbol{r}'')d^2\boldsymbol{r}'' = Cd^2\boldsymbol{r}'' \int_{\text{source}} d^2\boldsymbol{r} \; \cos^3\theta f(\boldsymbol{r}) g(a\boldsymbol{r}'' + b\boldsymbol{r}), \qquad (2.19)$$

where

$$C = \frac{T}{4\pi(s_1 + s_2)^2}. \qquad (2.20)$$

What we have achieved in Equation 2.19 is that we have written our image in terms of the x-ray source and the transmittance of the object that relates to the image and the x-ray source through the line of sight. The vector $a\boldsymbol{r}'' + b\boldsymbol{r}$ tells us where to evaluate the transmittance function g, which is precisely the location in the object plane through the line of sight between the source element $\boldsymbol{r}$ and the image element $\boldsymbol{r}''$. Equation 2.19 tells us how our image is composed and it gives us a hint of what we could learn about the object from our image.

It is possible to further simplify Equation 2.19. We are generally interested in systems where $s_1 + s_2$ is large compared to $|\boldsymbol{r}|$ or $|\boldsymbol{r}''|$. We can thus make the approximation $\theta \approx 0$ and $\cos^3\theta \approx 1$. Dropping the $d^2\boldsymbol{r}''$ factor from both sides, this leaves us with:

$$h(\boldsymbol{r}'') \approx C \int_{\text{source}} d^2\boldsymbol{r} f(\boldsymbol{r}) g(a\boldsymbol{r}'' + b\boldsymbol{r}). \qquad (2.21)$$

2.3.4   Reduction to a Convolution

Equation 2.21 is starting to resemble a convolution integral. We will now explore this resemblance further. We will try to write the integral in Equation 2.21 as over the image plane instead of over the source plane. To do this, we will need to project the f and g fuctions onto the image plane before integrating them over the image plane. Appropriate scaling of the f and g fuctions based on the geometry is needed. We define a new variable $\boldsymbol{r}_0''$, given by

$$\boldsymbol{r}_0'' = -\frac{s_2}{s_1}\boldsymbol{r} = -\frac{b}{a}\boldsymbol{r}. \qquad (2.22)$$

Multiplication of $\boldsymbol{r}$ by $-b/a$ is equivalent to projecting it through a point (the origin) in the object plane to the image plane, as illustrated in Figure 5. Thus, we can use $\boldsymbol{r}_0''$ to define a scaled version of f as $\tilde{f}$, the tilde

indicating *projection onto the image plane.*

$$\tilde{f}(\boldsymbol{r}_0'') = f(\boldsymbol{r}) = f\left(-\frac{a}{b}\boldsymbol{r}_0''\right) \tag{2.23}$$

$$\tag{2.24}$$

$$\boldsymbol{r}_O'' = -\frac{S_2}{S_1}\boldsymbol{r}$$
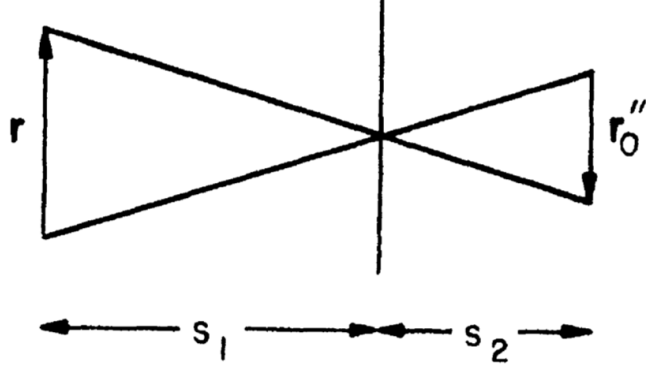
Figure 5: Illustration of $\boldsymbol{r}_0''$.

We can also use $\boldsymbol{r}_0''$ to define a scaled version of g as $\tilde{g}$, effectively projecting g from the object plane onto the image plane from a point in the source plane (defined by the vector $\boldsymbol{r}$).

$$\tilde{g}(\boldsymbol{r}_0'') = g(a\boldsymbol{r}_0''). \tag{2.25}$$

We can rewrite g in terms of these new variables:

$$g(a\boldsymbol{r}'' + b\boldsymbol{r}) = g(a\boldsymbol{r}'' - a\boldsymbol{r}_0'') = \tilde{g}(\boldsymbol{r}'' - \boldsymbol{r}_0''), \tag{2.26}$$

which leads to a final form for $h(\boldsymbol{r}'')$:

$$\begin{aligned} h(\boldsymbol{r}'') &= \left(\frac{a}{b}\right)^2 C \int_\infty d^2\boldsymbol{r}_0'' \tilde{f}(\boldsymbol{r}_0'')\tilde{g}(\boldsymbol{r}'' - \boldsymbol{r}_0'') \\ &= \left(\frac{a}{b}\right)^2 C\tilde{f}(\boldsymbol{r}'') ** \tilde{g}(\boldsymbol{r}'') \end{aligned} \tag{2.27}$$

where the ∞ subscript in the integral indicates integration over the entire 2D detector plane. By looking at the geometry carfully, it is reassuring to see that $\tilde{g}$ in the integral is evaluated at exact where it should be – through the line of sight connecting the source element and image element.

We have thus achieved our goal and described the detected photon density as the output of a 2D linear system with input $\tilde{f}$ and kernel proportional to $\tilde{g}$ (or equivalently, an input $\tilde{g}$ and kernel proportional to $\tilde{f}$). As

with any linear system, a frequency-domain description is very useful:

$$\mathscr{F}_2\left\{h(\boldsymbol{r''})\right\} = H(\boldsymbol{\rho''}) = (a/b)^2 C\tilde{F}(\boldsymbol{\rho''})\tilde{G}(\boldsymbol{\rho''}), \tag{2.28}$$

where $\boldsymbol{\rho''}$ is the spatial frequency vector conjugate to $\boldsymbol{r''}$ in the image plane. Recall the scaling relation for an nD Fourier transform:

$$\mathscr{F}_N\left\{f(\boldsymbol{r}/b)\right\} = |b|^N F(b\boldsymbol{\rho}). \tag{2.29}$$

We can use this to evaluate the right side of Equation 2.28 in terms of the original source and transmission functions f and g:

$$\tilde{F}(\boldsymbol{\rho''}) = \mathscr{F}_2\left\{f(-a\boldsymbol{r''}/b)\right\} = (b/a)^2 F(-b\boldsymbol{\rho''}/a) \tag{2.30}$$

$$\tilde{G}(\boldsymbol{\rho''}) = \mathscr{F}_2\left\{g(a\boldsymbol{r''})\right\} = (1/a)^2 G(\boldsymbol{\rho''}/a). \tag{2.31}$$

Our final result is then

$$H(\boldsymbol{\rho''}) = (C/a^2)F(-b\boldsymbol{\rho''}/a)G(\boldsymbol{\rho''}/a). \tag{2.32}$$

Recall that the double-primed coordinate represent the frequency vector in the image plane. By letting $\boldsymbol{\rho''} = a\boldsymbol{\rho'}$ and $\boldsymbol{\rho''} = -a\boldsymbol{\rho}/b$ we can also express Equation 2.32 in the object ($\boldsymbol{\rho'}$) and source ($\boldsymbol{\rho}$) planes as follows:

$$H(a\boldsymbol{\rho'}) = (C/a^2)F(-b\boldsymbol{\rho'})G(\boldsymbol{\rho'}) \tag{2.33}$$

$$H(-a\boldsymbol{\rho}/b) = (C/a^2)F(\boldsymbol{\rho})G(-\boldsymbol{\rho}/b). \tag{2.34}$$

In each of Equations 2.32, 2.33, and 2.34, the Fourier transform of the image is a product of the Fourier transform of the source and the Fourier transform of the object. In the image plane, the Fourier transform of the image is not scaled but the Fourier transform of the object is scaled and the Fourier transform of the source is both scaled and inverted as in its projection by a pin-hole camera. In the object plane, the object is not scaled. In the source plane, the source is not scaled. Proper scaling of the source, object, and image is important to make these equations work.

2.3.5 Image of the focal spot

The perhaps non-intuitive result of this analysis is that the x-ray source plays such an important role in the imaging chain. We have shown that the detected image can be modeled as a convolution of the object with the x-ray source – the source is thus always "in" the image, in a certain sense. We would like to characterize this effect in more detail. We recognize that the image of the x-ray source is really the point-spread function (PSF), and Equation 2.32 should convince us of that.

Let us model the x-ray source "focal spot" simplistically as a uniform, emissive disk of diameter d_{fs}, so the

emission function is

$$f(\boldsymbol{r}) = f_0 \text{ circ}\left(\frac{2r}{d_{fs}}\right),$$

(2.35)

where f_0 is the emission density (photons per unit area per unit time) within the disk region (see Figure 6). Recall that the "circ" function is defined as:

$$\text{circ}(r) = \begin{cases} 1 & r \leq 1 \\ 0 & \text{else} \end{cases}.$$
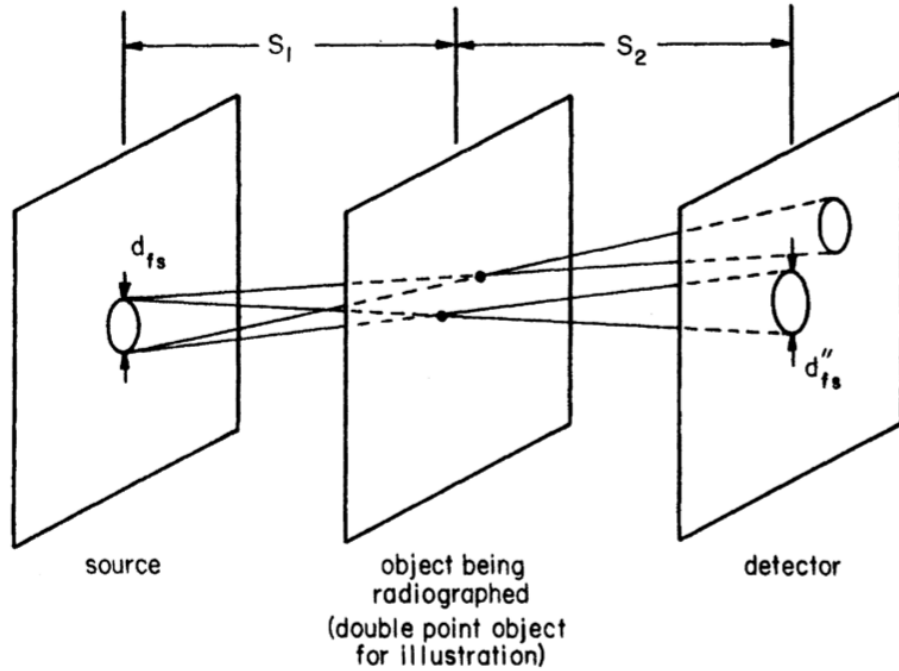
(2.36)

Figure 6: Diagram illustrating the calculation of the point spread function for transmission radiography with a disklike focal spot.

To find the image of the focal spot, and nothing else, we consider a point object input described by

$$g(\boldsymbol{r}') = \delta(\boldsymbol{r}' - \boldsymbol{r}'_1),$$

(2.37)

where $\boldsymbol{r}'_1$ is the location of the point in the object plane. The notion of a "point" transmission might seem counterintuitive – we are describing a hypothetical object that becomes "infinitely transmissive" over an infinitesimal area. You might consider a pinhole aperture with area approaching zero while the exposure time is increased proportionally. It should be clear now the image of this point object from the x-ray focal spot is just an image of the focal spot and the PSF.

10

Substituting Equations 2.35 and 2.37 into 2.21, we find

$$h(\boldsymbol{r}'') = C \int_{source} d^2\boldsymbol{r} f_0 \, \text{circ}\left(\frac{2r}{d_{fs}}\right) \delta(a\boldsymbol{r}'' + b\boldsymbol{r} - \boldsymbol{r}')$$

$$= \left(\frac{C}{b^2}\right) f_0 \, \text{circ}\left[\frac{2|a\boldsymbol{r}'' - \boldsymbol{r}_1'|}{bd_{fs}}\right]$$

$$= \left(\frac{C}{b^2}\right) f_0 \, \text{circ}\left[\frac{2|\boldsymbol{r}'' - (\boldsymbol{r}_1'/a)|}{bd_{fs}/a}\right], \tag{2.38}$$

where we have made use of the sifting property of delta functions. This equation describes a uniform disk image of diameter d_{fs}'', given by

$$d_{fs}'' = \frac{b}{a}d_{fs} = \frac{s_2}{s_1}d_{fs}. \tag{2.39}$$

This disk image of the disk focal spot is centered at $\boldsymbol{r}'' = \boldsymbol{r}_1'/a = \boldsymbol{r}_1'(s_1 + s_2)/s_1$, the magnification m_t is therefore $(s_1 + s_2)/s_1$. Note that m_t is always a positive number greater than 1.

Up to this point we have assumed the detector to be perfect. But Equations 2.32 tells us that if we model the detector as a linear system with a transfer function, it's easy to incorporate into our modeling a realistic detector through its transfer function. Let us denote the detector transfer function as $D(\boldsymbol{\rho}'')$. The detector output from input $H(\boldsymbol{\rho}'')$ is just $D(\boldsymbol{\rho}'')H(\boldsymbol{\rho}'')$. In the spatial domain, the input is $h(\boldsymbol{r}'')$ and the output is $h(\boldsymbol{r}'')$ convolved with the detection PSF. Using Equation 2.32, we can write this as

$$D(\boldsymbol{\rho}'')H(\boldsymbol{\rho}'') = (C/a^2)D(\boldsymbol{\rho}'')F(-b\boldsymbol{\rho}''/a)G(\boldsymbol{\rho}''/a). \tag{2.40}$$

We can rewrite this in the object plane so that the object spatial frequencies are not scaled, by letting $\boldsymbol{\rho}'' = a\boldsymbol{\rho}'$, as

$$D(a\boldsymbol{\rho}')H(a\boldsymbol{\rho}') = (C/a^2)D(a\boldsymbol{\rho}')F(-b\boldsymbol{\rho}')G(\boldsymbol{\rho}'). \tag{2.41}$$

$G(\boldsymbol{\rho}')$ now appears on the right side with no scaling. The overall transfer function of the system with respect to the object is thus given by the coefficient of $G(\boldsymbol{\rho}')$:

$$TF_{tot}(\boldsymbol{\rho}') = P_{tot}(\boldsymbol{\rho}') = (C/a^2)D(a\boldsymbol{\rho}')F(-b\boldsymbol{\rho}'), \tag{2.42}$$

which we can write in the spatial domain as

$$\text{PSF}_{tot}(\boldsymbol{r}') = p_{tot}(\boldsymbol{r}') = (C/a^2)\mathscr{F}_2^{-1}\left\{D(a\boldsymbol{\rho}')F(-b\boldsymbol{\rho}')\right\} \tag{2.43}$$

$$= p_{fs}(\boldsymbol{r}') ** p_{det}(\boldsymbol{r}'), \tag{2.44}$$

where $p_{fs}(\boldsymbol{r}')$ is the PSF due to the focal spot alone:

$$p_{fs}(\boldsymbol{r}') = (C/a^2)\mathscr{F}_2^{-1}\left\{F(-b\boldsymbol{\rho})\right\} = \left(\frac{C}{a^2b^2}\right) f\left(-\boldsymbol{r}'/b\right), \tag{2.45}$$

and $p_{det}(\boldsymbol{r}')$ is the PSF due to the detector:

$$p_{det}(\boldsymbol{r}') = \mathscr{F}_2^{-1}\left\{D(a\boldsymbol{\rho}')\right\} = (1/a^2)d\left(\boldsymbol{r}'/a\right). \tag{2.46}$$

These results confirm that the x-ray focal spot is indeed "n" every image, that the total system PSF is composed of the image of the focal spot convolved with the PSF of the detector.

2.3.6 Optimal Design Considerations

How do we decide on the geometrical aspect of our image system, namely, s_1 and s_2? Now that we have learned what the total system transfer function is composed of, we can explore how to optimize our system design.

Recall that the magnification is defined as

$$m_t = \frac{s_1 + s_2}{s_1} = \frac{1}{a} = \frac{1}{1-b}. \tag{2.47}$$

Equivalently, we see that

$$b = 1 - \frac{1}{m_t} = \frac{m_t - 1}{m_t}. \tag{2.48}$$

Applying these results to Equations 2.45 and 2.46, we see that

$$p_{fs}(\boldsymbol{r}') \propto f\left(\frac{-m_t\boldsymbol{r}'}{m_t - 1}\right) \tag{2.49}$$

$$p_{det}(\boldsymbol{r}') \propto d(m_t\boldsymbol{r}') \tag{2.50}$$

The width of $p_{fs}(\boldsymbol{r}')$ is smallest when the coefficient of $\boldsymbol{r}'$ of Equation 2.49 is the largest, which occurs when $m_t = 1$. That is, blurring from the focal spot is minimized in "contact" imaging ($s_2 = 0$), when the detector is in direct contact with the object being imaged, and there is no magnification. However, we see from Equation 2.50 that, to minimize blurring from the detector, a large magnification is needed. So the results of these design considerations are opposite to each other. Contact imaging is best to minimize the blurring effect of the finite size of the focal spot and magnification imaging is best to reduce the effect of detector blur.

It is possible to further optimize the choice of magnification if we make additional simplifying assumptions. Let us model the PSFs from the focal spot and detector as Gaussians. Recall that the Fourier transform of a Gaussian function is another Gaussian function. In the frequency domain then, we will assume that

$$D(\boldsymbol{\rho}'') \propto \exp\left[-\pi\left(\boldsymbol{\rho}''/\rho_d''\right)^2\right] \tag{2.51}$$

$$F(\boldsymbol{\rho}) \propto \exp\left[-\pi\left(\boldsymbol{\rho}/\rho_f\right)^2\right], \tag{2.52}$$

where ρ_d'' and ρ_f are characteristic widths of the MTF of the detector and focal spot, respectively. We find the overall MTF from Equation 2.42,

$$\mathrm{MTF}_{tot} = \frac{|P_{tot}(\boldsymbol{\rho}')|}{P_{tot}(0)} \propto \exp\left[-\pi(a\boldsymbol{\rho}'/\rho_d'')^2\right]\exp\left[-\pi(b\boldsymbol{\rho}'/\rho_f)^2\right]. \tag{2.53}$$

From Equations 2.47 and 2.48, this can be written as

$$\text{MTF}_{tot} = \exp\left[-\pi\boldsymbol{\rho}'\left(\frac{1}{(m_t\rho_d'')^2} + \frac{(m_t - 1)^2}{(m_t\rho_f)^2}\right)\right]. \tag{2.54}$$

The width of MTF_{tot} will be an extremum if

$$\frac{d}{dm_t}\left[\frac{1}{(m_t\rho_d'')^2} + \frac{(m_t - 1)^2}{(m_t\rho_f)^2}\right] = 0, \tag{2.55}$$

which has the solution

$$m_t^{opt} = 1 + \left(\frac{p_f}{p_d''}\right)^2. \tag{2.56}$$

We are interested in two limits of Equation 2.56. If we have a very large focal spot ($\rho_f \to 0$), then $m_t^{opt} = 1$, which, as we have already discussed, indicates contact imaging. On the other hand, if our detector is very poor ($\rho_d'' \to 0$), we require a large magnification. In other words, we can tolerate having a large focal spot by performing contact imaging, at the cost of having no magnification. This is generally what occurs, as the focal spot is often a more dominant contribution to the system PSF than the detector.

Note: this discussion on linear systems theory was adapted from Chapter 4 in Barrett [1]. Please read through the rest of that chapter for a more detailed analysis and insight into further design considerations.

3   X-ray Detectors

An ideal x-ray detector provides an unbiased estimate of the location, energy, and time of arrival of every incident photon at any rate of arrival. Throughout this section we will look closer at these requirements and see how real x-ray detectors fail to be ideal.

3.1   Quantum efficiency

The first task of any x-ray detector is to absorb all incident x-rays. We call the fraction of incident x-rays that interact in the detector the **quantum efficiency**, denoted by η. The quantum efficiency is related to the linear attenuation coefficient of the x-ray detector, μ, and the thickness of the detector t by

$$\eta = 1 - e^{-\mu t}. \tag{3.1}$$

An ideal detector will stop all x-rays, so we would like μt to be as large as possible. Therefore, an x-ray detector should be thick and made of a material with high atomic number. If the quantum detection efficiency is less than one, then the detector's SNR will be reduced by a factor of $\sqrt{\eta}$ and Eq. 2.8 becomes

$$\mathrm{SNR} = C\sqrt{\eta A \bar{\phi}}. \tag{3.2}$$

Recall from the Rose model that we need an SNR of approximately 5 to detect a signal. This means that reducing the quantum efficiency will require us to increase the incident x-ray fluence to maintain a fixed SNR. Increasing the photon fluence will increase the dose to the patient, so quantum efficiency is an important metric for x-ray detectors.

3.1.1 SNR

3.1.2 DQE

3.1.3 NEQ

3.2 Analog Detectors

3.2.1 Film structure

3.2.2 Optical density / H&D Curve

3.2.3 Important Film properties (speed, etc.)

3.2.4 Intensifying Screen

3.2.5 DQE of film

3.2.6 MTF of film

3.2.7 Physics modeling of Film (Ag grain density, etc)

3.2.8 Model of intensifying Screen PSF

3.2.9 MTF of Screen-Film

3.3 Digital Detectors

3.3.1 Intro

3.3.2 DQE

3.4 Analog Detectors

Analog images are acquired and displayed on film. Film consists of a plastic base coated with a gelatin binder that contains light-sensitive silver halide crystals. Figures 7 and 8 show schematic and scanning electron micrograph views of film.

When a photon hits a (transparent) silver halide crystal, a photochemical reaction occurs that creates two (opaque) metallic silver atoms. Under typical conditions the number of metallic silver atoms is far too small for the film to become visibly opaque to human eyes, but the film now contains a latent image in the form of silver atoms within silver halide grains. To make the image visible, we need to "amplify" the number of metallic silver atoms in each grain using a *developer solution*, then remove the unexposed silver halide crystals using a *fixing solution*. The result is a *photographic negative* that is dark (lots of metallic silver) in regions that have been exposed and light in regions that have not been exposed. In x-ray imaging the photographic negative is used directly, but in photographic imaging you need to invert the film brightness by projecting light through the negative, imaging the result on film, then repeating the development process. See [1, 2] for a more detailed discussion of the film development process.

For an x-ray film with a thin coat of silver halide grains, the grain size determines the spatial resolution. Film grains are approximately 0.2-2 μm in diameter which gives us a sense of the smallest resolvable feature. For comparison a typical 2018 scientific CCD has a pixel width of 6 μm and an iPhone X display has a pixel width of 55 μm. Film has unmatched spatial resolution even in 2018.

Only a few percent of incident x-rays interact as they pass through film. Because quantum efficiency is so important for medical imaging, most medical x-ray film uses a photographic emulsion coating on both sides of the plastic base. We could increase the thickness of the emulsion layers to improve quantum efficiency further, but this would reduce spatial resolution and make developing the film more difficult.

We can improve the quantum efficiency of film by placing a *fluorescence screen* directly on the film. Fluorescence screens have a high attenuation coefficient and contain an x-ray phosphor that converts incident x-rays into many visible (plus infrared and ultraviolet) photons. These visible photons expose the film and the film can be developed normally. Unfortunately, the visible photons do not travel straight to the film along their generating x-ray's path—they spread out before they reach the film. This means that using a fluorescence screen improves quantum efficiency at the expense of spatial resolution. This type of detector is often called an *indirect analog* detector because it indirectly detects the incident x-rays.
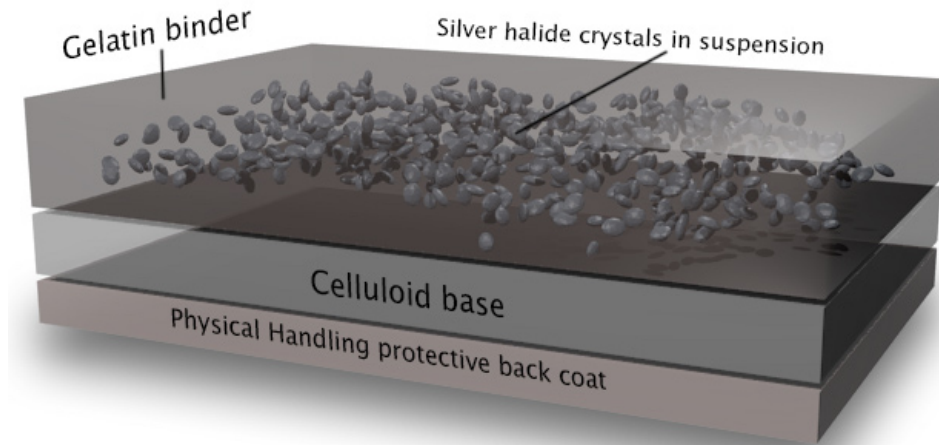

Figure 7: Schematic view of photographic film. [2]

The input to a film detector is the x-ray exposure measured in coulombs per kilogram (C/kg) or röntgen (R). The output of a film detector is usually measured with a unitless property called optical density (OD). If a thin beam of light with intensity I_0 hits the film and the transmitted beam has intensity I, then the optical density of the film at that point is defined as

$$OD = -\ln\left(\frac{I}{I_0}\right).\tag{3.3}$$

A high OD means that the film is opaque which corresponds to a high x-ray exposure. The relationship between x-ray exposure (input) and optical density (output) is often called the *characteristic* curve, the *Hurter-Driffield* curve, or the D—$\log E$ curve. An example of a characteristic curve is shown in Fig. 9. Note the often confused units on the characteristic curve—the horizontal axis uses a logarithmic exposure scale and the vertical axis uses a linear scale for optical density which is itself a logarithm of the input-output intensity ratio (see Eq. 3.3).

Let's examine the features of the characteristic curve in Fig. 9. When the film has not been exposed the optical density is not zero—even unexposed film is not completely transparent due to reflections, impurities, and thermal effects. As we start to expose the film, we begin to create metallic silver atoms. A single metallic silver atom in a grain is not enough to create a latent image though; about 4 metallic silver atoms are required
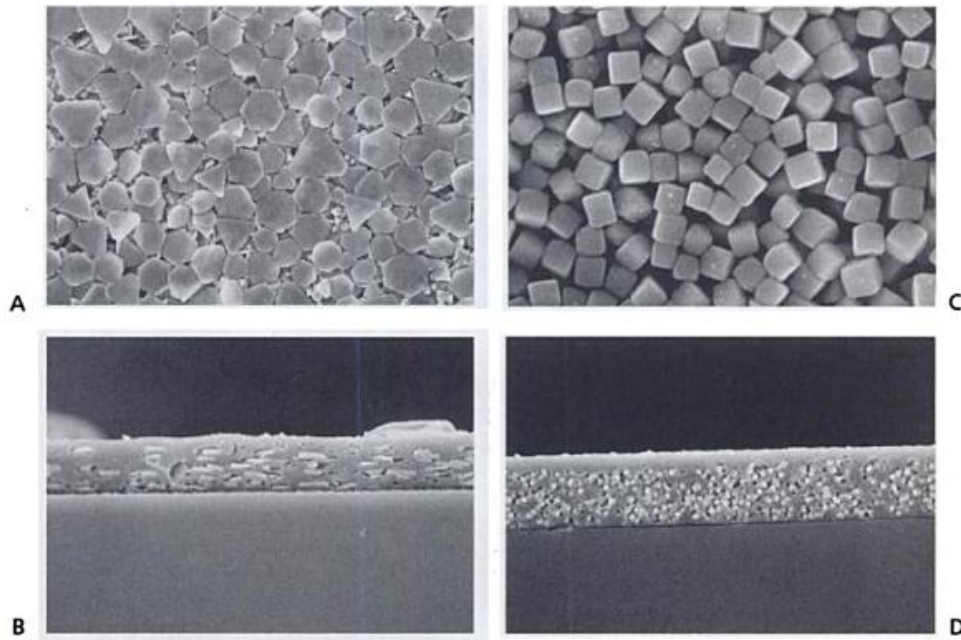
Figure 8: Scanning electron micrographs (SEM) of photographic film. **A**: A top-down SEM image of the emulsion layer of T grain emulsion. **B**: A cross section of the T grain emulsion film showing the grains in the gelatin layer supported by the polymer film base below. **C**: Cubic grain film emulsion in a top-down SEM view. **D**: Cross section of the cubic grain film. SEM courtesy of Drs. Bernard Apple and John Sabol. Citation needed.

in a single grain to ensure that it will be developed. This means that for low exposures the optical density will increase slowly—this is evident in the "toe" of the characteristic curve. At high exposures most of the grains in the film already have many metallic silver atoms, so increasing the exposure will not increase the optical density further—this is evident in the "shoulder" of the characteristic curve. Finally, at intermediate exposures the optical density increases linearly with the log exposure. The slope of characteristic curve is often called the *speed* of the film because it summarizes how quickly a fixed exposure rate will increase the optical density—this terminology is borrowed from photographers who will use a "fast" film in situations where they require short exposure times e.g. sports photography. See [1] chapter X for a complete derivation of film's characteristic curve.

The characteristic curve also depends on the film processing conditions which can vary significantly. The proportions of chemicals in the developer solution and the temperature will affect the shape of the characteristic curve and the speed point. Care is taken to keep the chemistry and the temperature of the developer as constant as possible.

Film's characteristic curve also depends on the exposure rate. The metallic silver atoms in each grain are unstable and will re-ionize back into the silver halide crystal over time. If the exposure rate is very low, then these re-ionization events can significantly reduce the number of developable grains which will reduce the OD in the final image. In other words, the characteristic curve will shift to the right for low exposure rates. This property of film is often referred to as *reciprocity law failure* or the *Schwarzschild effect* after Schwarzschild noticed the issue while imaging dim stars.
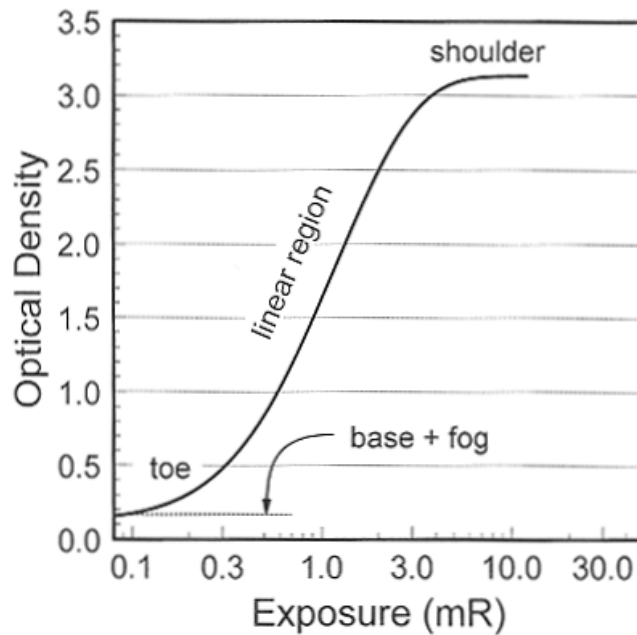
17

Figure 9: A characteristic curve for film. Notice the logarithmic scale on the horizontal axis and the linear scale on the vertical axis.

3.5 Digital Detectors

We will briefly discuss several types of digital detectors and leave the details for Patrick's lectures. The defining feature of a digital detector is that its output is a digital signal with discrete values. Digital images are usually displayed electronically, but they can be also printed on film. Thus, the acquisition of the image is separate from the display of the image and each component can be optimized separately. The input to a digital detector is exposure, and the output is a pixel value (PV). Digital systems usually respond linearly to x-ray exposure.

Indirect digital detectors use a phosphorescent screen (often CsI) coupled to a charge-couple device (CCD) camera or a think-film transistor (TFT) water. Incident x-rays are converted to visible photons in the screen which generates a signal in the CCD. Indirect digital detectors are analogous to indirect analog detectors.

Direct digital detectors use materials that produce electron-hole pairs that can be collected directly. Selenium (Se), amorphous silicon (a-Si), and cadmium zinc telluride (CZT) are common materials for direct digital detectors. An electric field is applied across the width of the detector and the electron-hole pairs follow the field lines that are perpendicular to the surface of the detector where they are collected and read out.

Photon counting detectors can measure individual x-ray interactions. Some direct digital detectors can act as photon-counting detectors. Non-photon counting detectors integrate quanta (photons or electrons) over the total exposure time of the image acquisition.

Computed radiography (CR) detectors store a latent image as electrons trapped in a phosphor screen (usually BaFCl). The electrons are subsequently read out by scanning the phosphor with a laser beam. The laser light stimulates the trapped electrons back into the conduction band where they can return back to the valence band with the emission of light. The emitted light is collected to create a digital image. These detectors use the same principle as optically stimulated luminescent dosimeters (OSLD) in radiation dosimetry.

4 X-ray Image Quality

In this section we will introduce the basics of x-ray imaging and develop three tools that we can use to quantify image quality—contrast, resolution, and noise. We will focus on x-ray imaging in these notes, but these tools are useful for analyzing all imaging modalities.

4.1 Review of useful concepts

4.1.1 Central-limit theorem

4.1.2 Gaussian random variable

4.1.3 Poisson statistics

4.1.4 Stationarity

4.1.5 Ergodicity

4.1.6 Ensemble average

4.2 Resolution

4.2.1 Signal transfer / linear system model

4.3 Noise

4.3.1 Noise transfer (autocorrelation, NPS)

4.4 Contrast

4.4.1 Rose Model

4.5 The effect of Scatter

4.5.1 Resolution: Scatter psf

4.5.2 Contrast: Rose Model

The derivation of expressions for contrast and SNR under the Rose model in section 2.2 neglected the effects of scattered radiation. In general, scattered radiation always works to decrease the contrast and overall quality of an image, as seen in Figure 10. This effect can be quantitatively demonstrated with a simple extension of the Rose model.

Recall our previous definition of contrast under the Rose model,

$$C = \frac{\Delta\phi}{\bar{\phi}} = \frac{\phi_1 - \phi_2}{(\phi_1 + \phi_2)/2} \tag{4.1}$$

Referring to Figure 11, we can define a "no scatter" contrast, C_{NS}, accounting only for contrast from the primary fluence components, ϕ_{1p} and ϕ_{2p}, That is,

$$C_{NS} = \frac{\phi_{1p} - \phi_{2p}}{(\phi_{1p} + \phi_{2p})/2} = \frac{\phi_{1p} - \phi_{2p}}{P} \tag{4.2}$$

where we define P as the mean primary fluence, $(\phi_{1p} + \phi_{2p})/2$.
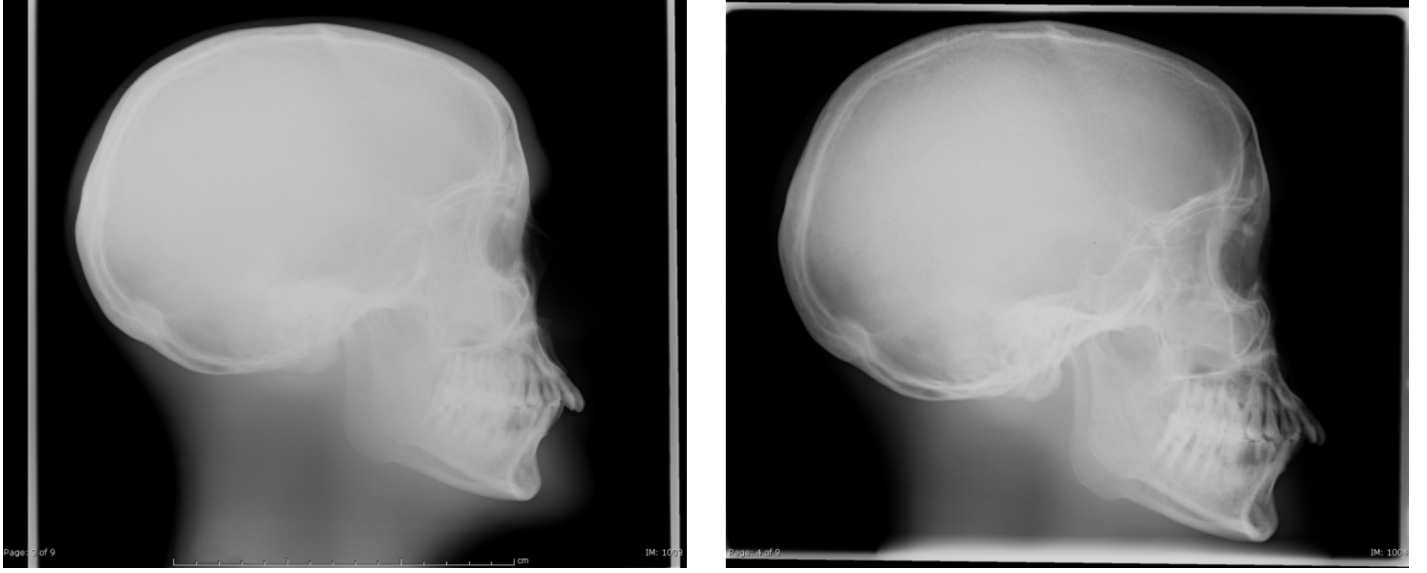
Figure 10: Left: Radiograph of the skull with contrast. Right: Radiograph of the same skull with an anti-scatter grid in place. Note the improvement in image contrast.

Likewise, we can define a "scatter" contrast, C_S,

$$C_S = \frac{(\phi_{1p} + \phi_{1s}) - (\phi_{2p} + \phi_{2s})}{[(\phi_{1p} + \phi_{1s}) + (\phi_{2p} + \phi_{2s})]/2} \tag{4.3}$$

$$= \frac{(\phi_{1p} - \phi_{2p}) + (\phi_{1s} - \phi_{2s})}{[(\phi_{1p} + \phi_{2p}) + (\phi_{1s} + \phi_{2s})]/2} \tag{4.4}$$

$$\tag{4.5}$$

If we assume that the scatter component of each fluence is roughly equal, that is $\phi_{1s} \approx \phi_{2s} = \phi_S$, and define $S = \phi_S$, then C_S can be written

$$C_S = \frac{\phi_{1p} - \phi_{2p}}{P + S} \tag{4.6}$$

and we see that scatter reduces contrast.

We can relate the scatter and no-scatter contrasts as follows:

$$C_S = \frac{\phi_{1p} - \phi_{2p}}{P + S} \left(\frac{P}{P} \right) \tag{4.7}$$

$$= C_{NS} \left(\frac{P}{P + S} \right) \tag{4.8}$$

$$= C_{NS} \left(1 - \frac{S}{P + S} \right) \tag{4.9}$$

$$= C_{NS}(1 - \text{SF}) = C_{NS} \left(\frac{1}{1 + S/P} \right) \tag{4.10}$$

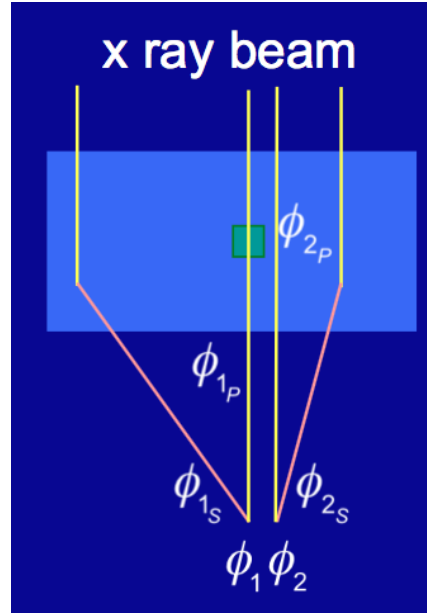using the scatter fraction:

$$\text{SF} = \frac{S}{P + S} \tag{4.11}$$

20

Figure 11: Rose model with scatter.

and scatter-to-primary ratio, S/P.

4.5.3 Anti-scatter grids

5 Image Interpretation

5.1 Six levels of Efficacy

5.2 The Ideal Observer

5.3 Mathematical Observers

5.3.1 Pre-whitening filter

5.3.2 Matched filter

5.3.3 Wiener filter

5.4 Human observers

5.5 Model observers

6   Conclusion

References

[1] Harrison H. Barrett and William Swindell. *Radiological imaging : the theory of image formation, detection, and processing.* Academic Press, New York, 1981. `https://doi.org/10.1016/c2009-0-02376-9`.

[2] `https://chemistry.stackexchange.com/a/59925`, 2016. [Online; accessed 11-April-2018].